Lab 3
Kaleidoscopic Anisotropy
An AMR Based Compass

Pavlo Milo Manovi

March 20, 2014

Contents

1 Introduction

The purpose of this lab was to introduce the Anisotropic Magnetoresistive sesnor and the effect that magnetism can have on sensors and sensor circuits. We were expected to use the HMC1022 AMR magnetometer to create a compass, with a mobile application in mind. A short review of how AMR sensor work and requisite knowledge for the construction of such a device are described in section two of this report with results discussed in section three.

2 Methods

2.1 Design Overview and Systems Level Analysis

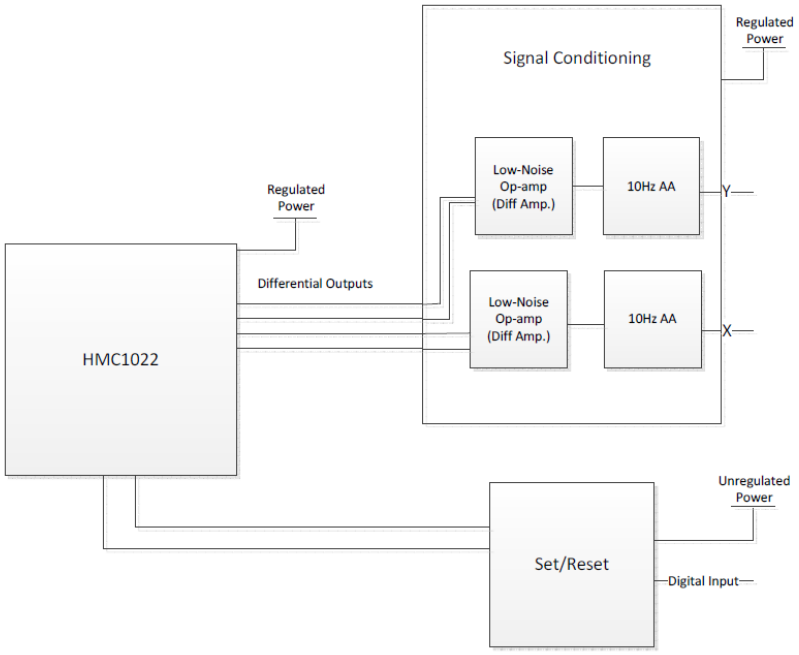

Figure 1: System Level Overview

Developing a robust and accurate compass system using the hmc1022 with mobile applications in mind required an understanding of the systems which would make up the circuit. Developing the compass as disjointed analog hardware and supporting digital software/hardware allowed for a clear understanding of what would be needed both a testing environment and in a mobile application while enabling flexibility in the supporting software algorithm development.

The decision to separate the compass hardware from any data acquisition and computation harware allowed for better emf and magnetic coupling control over the design during prototyping. In addition to better control over the physical aspects of the design, making the analog front-end a modular component allowed for the more difficult analog circuit design to not need to depend on the concurrent design of the supporting digital system. A system level overview of the analog component of the circuit can be see in in Figure 1.

Specifically the system would require power for both the sensing analog components, and the set/reset logic. As is the case in most mobile settings a battery is usually used to provide power to the system which has a voltage which decays with time as it is depleted of charge. As there are many voltage references and offsets required in this circuit which are a function of their supply voltage, the output of the system would change dramatically with time. To mitigate this problem, a stable LDO would need to be used to drop down a common battery voltage to a set voltage through the operation of this device to battery depletion.

It was assumed that in this application a single 3.6v (nominal li-po cell voltage) battiery would be used to power the device with a fully charged supply voltage of 4.2 volts, giving an operating range of 4.2-3.6V. Such a range allowed for a set-reset circuit to operate with 500mA spikes while also providing a voltage source above the minimum dropout voltage before battery cut-off for most LDOs. Running the regulated voltage at 3.3 volts for maximum compatibility with microcontrollers meant that a 3.6 - 4.2V supply would also waste less heat than a system running with a higher supply voltage, as LDOs become much less efficient as the differential between input voltage and output voltage increases.

In this design, strict separation of analog and digital components was not required as during high-current set/reset events which would cause spurrious readings the system would not be acquiring data from an ADC, allowing for the high-current set-reset circuit to sit anywhere on the board.

As the output of the HMC10xx series AMR magnetometers are all from opposing points of a wheatstone bridge a differential op-amp is required on the output of each AMR die. The HMC1022 has a sensitivity after a set/reset pulse at 500mA of 1.0 mV/V/gauss. Given that the earth's magnetic field flux density is usually weakest at 25μT the expected output swing should be $\frac{3.3v}{.25G}$, or .825mV, with a full range of twice that given the opposing easy axes in the AMR bridge elements and bridge output (to be discussed later in this lab writeup). Given that the output swing is only 1.65 mV, a differential op-amp was a necessity in the design of the signal conditioning portion of the compass circuit.

While many differential op-amp configurations exist, an impedance matched single op-amp difference amplifier will suffice. As in the end it is only the ratio of the two X and Y inputs which matters, large amounts of gain are not necesary as long as mo more than a tenth of a degree accuracty is required. While a three op-amp instrumentation amplifier would remove the need for matched input impedances, and provide less of a DC offset, the mean values of each of the AMR bridge outputs will be removed during compass calculations meaning that a constant DC offset due to the method of amplification won't matter much. A choice of a low-noise TL974 would suffice in the design, especially considering the relatively low-impedance of the AMR bridge resistances (specifics discussed in section 2.2.1).

A virtual ground reference at one half of the analog voltage source was also implemented to act as a virtual ground in the difference amplifier.

2.2 Electrical Design Implementation

2.2.1 Choice of Electrical Components

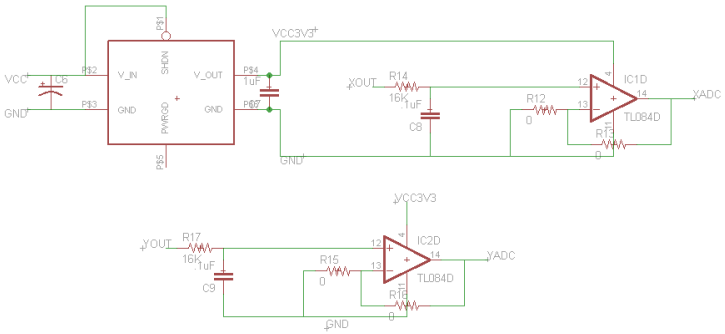

Figure 2: Voltage Regulation/Decoupling and Anti-Aliasing Filters

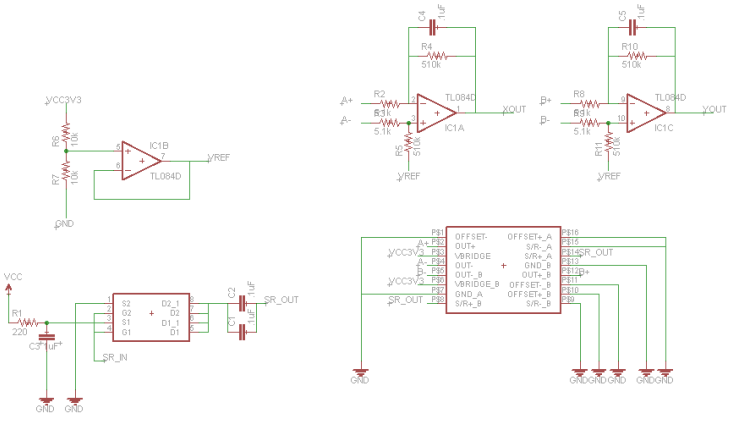

Figure 3: Difference amplifiers and voltage reference for virtual ground.

LDO: The MCP1826 was chosen for its low quiescent current of 120μA, its power-good output, its size, its price, and its low ouput capacitance requirement for stabilization. In a mobile application low quiescent current will yield a higher operating life off of a single battery charge given a sleep state, and using the power-good output of the LDO which will be valid as long as Vin is greater than 3.65 volts removes the need for additional battery

discharge voltage sensing for battery undervoltage lockout.

Op-Amp: The TL974 is a rail-to-rail op-amp which operates with -2.5 and 2.5 volt inputs, has a very low quiescent current, and a noise level of only $4\frac{nV}{\sqrt{Hz}}$ at 1000Hz. While it also boasts a low distortion of .003%, as the bandwidth of the signals of interest are around ten Hz this is relatively uninportant. Given that the TL974 was to be used as a differential amplifier, use of the TL974 allows for a gain of 60dB at a frequency of 1000Hz, giving a large amount of headroom for amplification in the first stage. Additionally, the TL974 has an offset voltage of 1mV, a value low enough to remove digitally during the heading calculation process. In a quad op-amp package the unit cost in quantities of ten is .83 cents, a very fair price for the characteristics it provides.

AOP605: A CMOS pair capable of sinking and sourcing 6.5 amps at 30V. As the set reset circuit requires both a pmos and nmos fet, using the AOP605 simplifies the circuit by requiring only one discrete component for the switching elements.

2.3 Board Layout

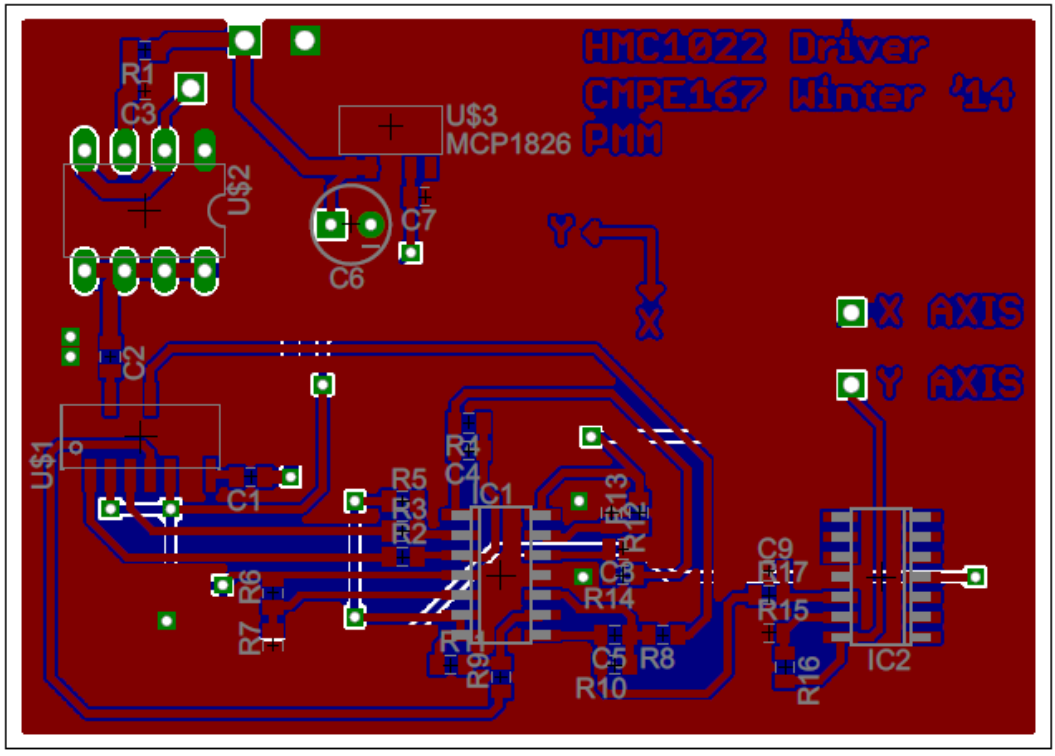

Figure 4: Compass Board Layout

As strict analog and digital segrigation was not required for this board, the layout was faily simple. As a habit I placed the high power and power regulation components in their own portion of the board. A large tank capacitor was included on the LDO output to help reduce noise during high slew-rate output events.

2.3.1 Set Reset Circuit

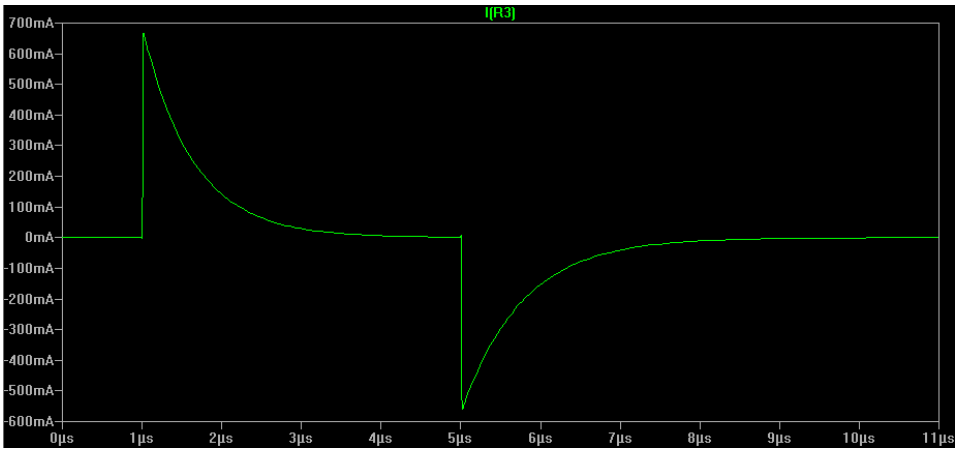

Figure 5: Spice Simulation of SR circuit with an input voltage of 3.65v.

The set/reset driving circuitry required to perform the actions of S/R as described in section 2.4 of this report as described in Honeywell's AN213 application note[1] delivers a positive or a negative current pulse through the set/reset straps of the AMR die. The bottom right circuit in figure 3 shows the schemtaic used which is set up for 2μS pulses through use of an RC circuit at the top of the totem pole. Operation of the set/reset circuit is achieved through a LVTTL logic level input to the gates of the totem pole. When the input voltage is high, the N channel mosfet is on and grounds the capacitors in series with the set/reset straps. When the input voltage transitions from high to low, the P channel mosfet turns on, the N channel mosfet turns off and the R-C circuit gets pulled towards VCC. Transitioning between sinking and sourcing potential charges the capacitors with a time constant determined by the strap and resistance of R1. As the initial transient will present itself as a decaying voltage across the straps, positive and then a negative current will flow, given a pulsetrain into the gate inputs of the circuit. A SPICE simulation of this model at the lowest operating voltage the compass circuit will operate at can be seen in figure 4.

2.3.2 Difference Amplifier

The gain for a differential amplifier is given as:

$$V_{\text{out}} = \left(\frac{R_1+R_f}{R_1}\right) \cdot \left(\frac{R_g}{R_g+R_2}\right) V_2 - \frac{R_f}{R_1} V_1.$$

[1] Totem Pole S/R circuit from page six of the application note was used.

Which means that in the case of the differential op-amp set up implemented in my compass, the total gain is equal to 100 (40dB and well under the 60dB max), as the impedance matched inputs are equal to 5.1k with 1% tolerance and the feedback and pulldown resistors are equal to 510k with 1% tolerance. Additionally, a .1μF capacitor is included in the feedback path of the op-amp, creating a low-pass filter with a cut-off of frequency of $\tilde{1}$9.5Hz.

Given an input differential of 1.65mV the output gain should be equal to .165 volts, or 819 LSB's on a 14 bit ADC, an effective 9.678 bits of resolution not considering any input noise.

2.4 Set/Reset Straps

The HMC1022 used in the design of my compass was manufactured with a Permalloy film as a magnetoresistive element. The film in any given HMC1022 when freshly manufactured has all of its component particles' magnetic domains aligned. In the case of the HMC102X family, this alignment can be disrupted by magnetic fields greater than 20 gauss; to put this into perspective, neodymium iron boron magnets or power conducting wires carrying large amounts of current can routinely create magnetic fields with strengths up to two orders of magnitude larger than 20 gauss. As fields with a flux density greater than or equal to 20 gauss are fairly common, a way of realigning the magnetic domains is required. This is the function of the Set/Reset straps.

The Set/Reset strap offers the ability for one to place the sensor in its most sensitive, linear state, and to flip the direction of the easy-axis of the sensor for use in offset calculation and calibration. To understand how exactly the Set/Reset straps can reorient the magnetic domains of the Permalloy particles, the construction and orientation of the Permalloy bridge elements must be explored.

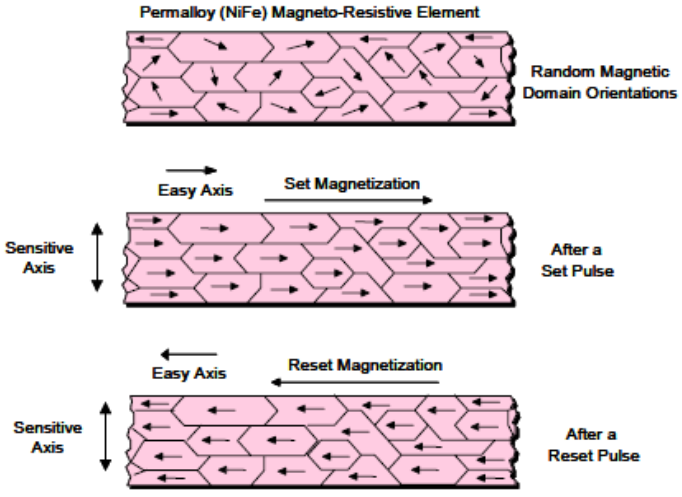

Figure 6: Anisotropic Magnetoresistive Die

2.4.1 AMR Bridge Construction

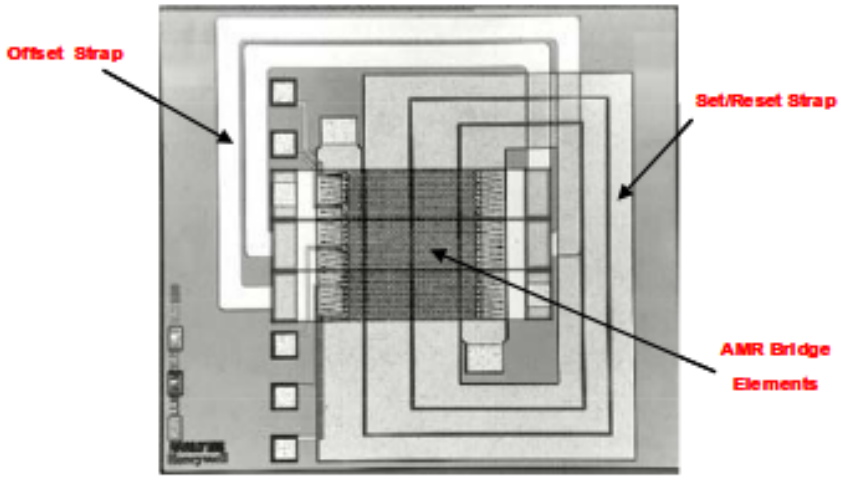

Figure 7: Anisotropic Magnetoresistive Die

Figure 5[2] is a photo of one of the two AMR die within the HMC1022. Two conductive paths can clearly be seen in the lithograph, labeled the Set/Reset Strap, and the Offset Strap. These two straps run orthogonally to the path of the AMR bridge elements and allow for a current to pass through them, and a resultant magnetic field of uniform direction to pass through the AMR bridge elements, magnetizing and re-orienting the Permalloy particles.

Figure 6 depicts resistive Permalloy elements aligned such that they all share a common axis. AMR sensors are defined by their dependance of electrical resistance of the angle between the direction of electric current and direction of magnetization.[3] As such, sharing a common sensitive axis allows for a positive voltage change with increating magnetic fields in the direction of the sensitive axis. Knowledge of the magnitude of the magnetic field along multiple axis allows for the derivation of the direction of any arbitrary magnetic field, the calculations required are explained under section 2.7 of this report.

[2]From Honeywell AN213 page 2.

[3]W. Thomson, Proc. Royal Soc. London,Vol. 8, (1856-1857), pp.546-550. – Discussion of anisotropic magnetoresistance.

2.4.2 AMR Bridge Configuration

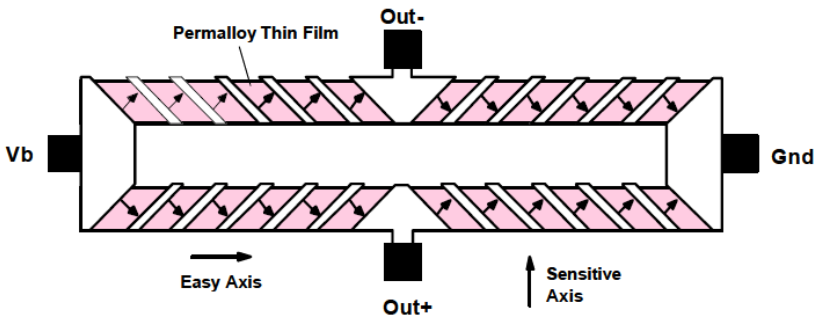

Figure 8: Magneto-Resistive wheatstone bridge elements.

The AMR sensor in all HMC10xx devices depicted in Figure 7[4] is designed as a wheatstone bridge. Using two half-bridge voltage dividers with identical equal resistances at a point when the sensor has no stiumulus allows for the expected voltage across the dividers to be one half of the total input voltage with a differentail voltage difference between the two bridge output points of zero. As the permalloy film strips are wrapped orthogonally to their bridge mates, as the field moves to be in alignment with the sensitive axis of the permalloy strip it moves out of the sensitive axis of the other, creating a bridge resistance offset, creating a voltage difference that's either negative of positive, allowing for differential amplification.

One of the downsides of using a wheatstone bridge for an AMR sensor is the fact that changes in output when measuring the Earth's magnetic field can be as small as 1.65mV, given a mismatched bridge impedance of one ohm on a nominal 1100 Ohm on a 5v supply (typical for the HMC102x), the offset voltage can be -2.27mV, which when amplified can cause large errors of many degrees. However, as the bridge resistances change relatively linearly with temperature and stay approximately constant over the life of the part, the offset can be subtracted from the final output.

Voltage offset for a wheatstone bridge is given as:

$$V_{off} = V_b(\frac{R2}{R1+R2} - \frac{R4}{R3+R4})$$

2.5 Noise Characteristics

2.5.1 Total Cascaded Noise

Each channel in the system X, and Y will have a total amount of noise given by the sum of all the noise generating components before it limited in bandwidth as per Friis formula for noise where G is the total power gain and F is the noise figure.

[4]Page six of the HMC10xx datasheet.

$$F_{total} = F_1 + \frac{F_2 - 1}{G_1} + \frac{F_3 - 1}{G_1 G_2} + \frac{F_4 - 1}{G_1 G_2 G_3} + ... + \frac{F_n - 1}{G_1 G_2 ... G_{n-1}}$$

A property of Friis equation is that the bandwidth of any noise creating element is limited by that before it as any spectral power attentuated by a previous circuit element is unable to attribute to the total noise figure in the circuit element after it.

Using a differential op-amp circuit noise model given in figure eight, the total combined root mean square resistor noise and op-amp noise is given by the following equation, where e represents voltage, i_w represents the current noise specification, and e_w represents the voltage noise specification for a given op-amp.[5].

$$V_{rms} = \sqrt{\frac{f_h}{f_l} 8kTR_2A + 2(i_w^2 R_2^2)(f_{inc} In2 \frac{f_h}{f_l}) + e_w^2 A^2 (f_{enc} In2 \frac{f_h}{f_l})}$$

The HMC1022 has a noise equivalence which is almost identical to the johnson noise of the bridge resistances, given by $\sqrt{4k_B T \Delta f R}$ which is equivalent to 18nV RMS given room temperature and a bandwidth of 20Hz. Without considering the effective bandwidth after the diff amps, using the full 5MHz bandwidth of the sensor, the highest amount of RMS noise voltage would be equal to 9.51μV.

Now, applying the op-amp noise equation and combining it with the noise coming out of the HMC1022 as per Friis equation yields a noise figure of approximately 2.54244μV + 18nV equal to 2.56μV, well under a single LSB of 201μV for a 14 bit sampling ADC.

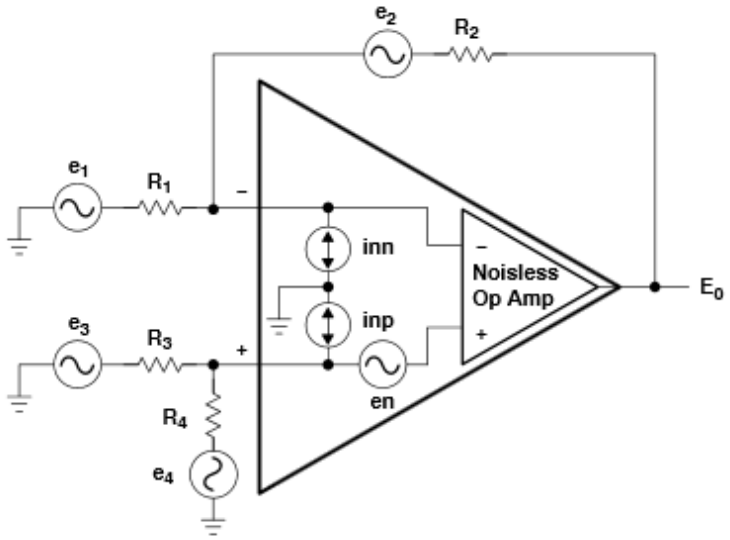

Figure 9: Difference Amplifier Noise Model

[5]Step by step noise analysis via superpositioning explained in TI's 'Differential Op Amp Circuit Noise Calculations' app note starting on page 14. http://www.ti.com/lit/an/slva043b/slva043b.pdf Additional information was obtained from analog device's MT-049 differential op-amp noise analysis app note.

2.5.2 Quantization Noise

Using a 14 bit ADC should yield a maximum signal to noise ratio of approximately 6.02*14 + 1.76 dB, or 86 dB. As the signal of each magnetometer output after filtering should be 47.4 dB above the noise introduced by op-amp and johnson noise, and the effective number of bits of my sampling circuit is 9.678, the actual SNR of the circuit is 59.495 dB, which is still sufficient.

2.6 Cross Axis Error

As the AMR sensors are manufactured as wheatstone bridges and the resistive elements are not only sensitive to one axis, but also slightly sensitive to an orthogonal axis (easy vs sensitive axis in figure 7), the effective output of the sensor will be skewed as a result of this sensitivity.

2.6.1 Compensation

Compensation of cross-axis effects can be achieved either though characterization of each axis using a Hemholtz coil in a zero-gauss chamber, or by using a large sample set to create a statistical model of the standard cross-axis effects. Both methods provide engineers with a constant offset which one needs to subtract from the X and Y readings to remove the skew which creates cross-axis effects.

As honeywell has done a large characterization of the magnetometers they produce[6], they provide the fact that given a full scale of 4 gauss, with set/reset usage and a field flux density of .25 gauss, at least a .3% offset should be expected on the output of both the X and Y AMR bridge. This can be subtracted digitally during the heading calculation process to get compensated values.

2.7 Heading Calculations

Each output is a representation of the magnetic field strength in the direction of the sensitive axis of the AMR sensor. Using multiple sensors with orthogonal sensitive axis allow for measurement of the magnitude and direction of any magnetic field using basic trigonometric relations. Figure 11 shows a portion of a MATLAB script used to translate X and Y values into heading readings.

[6]See honeywell AN205 for specific Cross-Axis Field Effects for different full range cross axis effects

```
for temp = 1:length(heading)
    if Y(temp) > 0
        heading(temp) = 90 - (atan(X(temp)/Y(temp)))*180/pi;
    end
    if Y(temp) < 0
        heading(temp) = 270 - (atan(X(temp)/Y(temp)))*180/pi;
    end
    if Y(temp) == 0 && X(temp) < 0
        heading(temp) = 180;
    end
    if Y(temp) == 0 && X(temp) > 0
        heading(temp) = 0;
    end
end
```

Figure 10: Trigonometric Heading Calculations

2.8 Data Acquisition Method

Data acquisition was achieved through the use of a USB-6009 DAQ and MATLAB using its data acquisition library. Data was oversampled at a rate of 2 kHz and filtered with a running FIR filter with a frequency cutoff set at 10Hz (determined by the anti-aliasing filter present in the circuit). As the most accurate results are obtained directly after the use of a set/reset strap, the data acquisition script I wrote in MATLAB toggled the set/reset strap using a digital output pin with a high signal time of 4μS, allowing for the full set transient to decay before taking a sample. The set/reset strap sequence was set to the anti-aliasing cutoff frequency of 10Hz. In this configuration, the highest possible linearity and repeatability (without the use of the offset straps) is achieved at the trade-off of amount of energy consumed.

2.9 Set/Reset Mobile Application Considerations

As each set/reset cycle requires dumping charge through the set/reset strap an analysis of the amount of charge it dissipates is required to better understand the effect of its use in an application with a finite amount of charge available.[7] An analysis of the amount of energy used in each set/reset even is a more intuitive approach as while the Set/Reset circuit draws many hundreds of mA, it does so only for a very short period of time.

$$\text{Energy Equation: } E = \frac{CV^2}{2}$$
$$\text{Using Set/Reset Values Used: } E = \frac{2E{-}7{*}4.2}{2}$$
$$E = 35.28erg$$

If a li-po battery with 1Ah of charge were to drive a compass module's set/reset circuitry which draws 70.56 erg per s/r, there would be 4.2 billion resets available before the battery became depleted of charge. At a rate of 10Hz with the method described in the previous section of this report, the compass s/r circuit would be able to run for 1.357 years.

[7] A good discussion on how to do this is available from Honeywell's AN213 on page 4.

3 Results

3.1 Observed Noise

In all indoor environments tested, the X and Y outputs to the DAQ had a peak to peak noise mean of 1.832mV and 1.916mV with a standard deviation of 1.3mV and 1.35mV for X and Y. These measurements were obtained using the data from ten seconds of data obtained at a rate of 2 GigaSamples per second with an HP Infineon Oscilloscope. An FFT of this data showed no large sources of noise from 60-120 Hz from the mains. As the LSB of this system is 200μV, this noise is visible in the acquired data, though attentuated through use of a FIR filter.

3.2 Discussion of Data

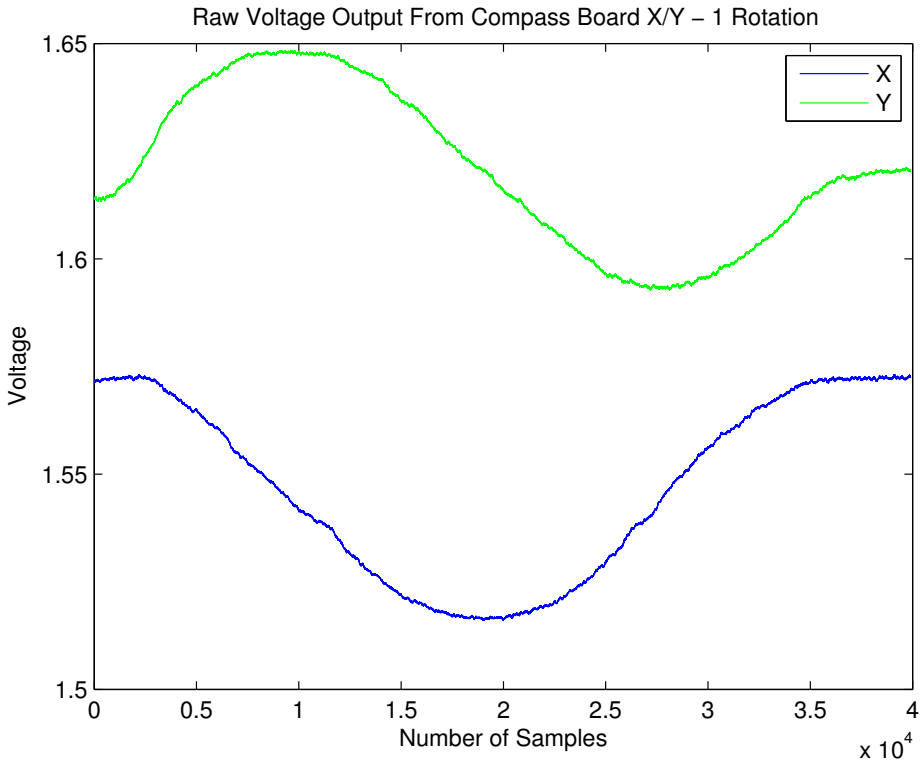

Figure 11: Conditioned X/Y Die Voltages With Offset

Figure 12 represents the voltages seen at the the X/Y output of the compass circuit. The compass was made to be level and rotated 360 degrees. The blue and green curves represent the X and Y output voltages of the compass with the offsets still intact. Variations in the AMR wheatstone die bridge arms and dc offsets from the op-amp as well as cross-axis errors all attribute to the 100mv difference in offset voltages between X and Y.

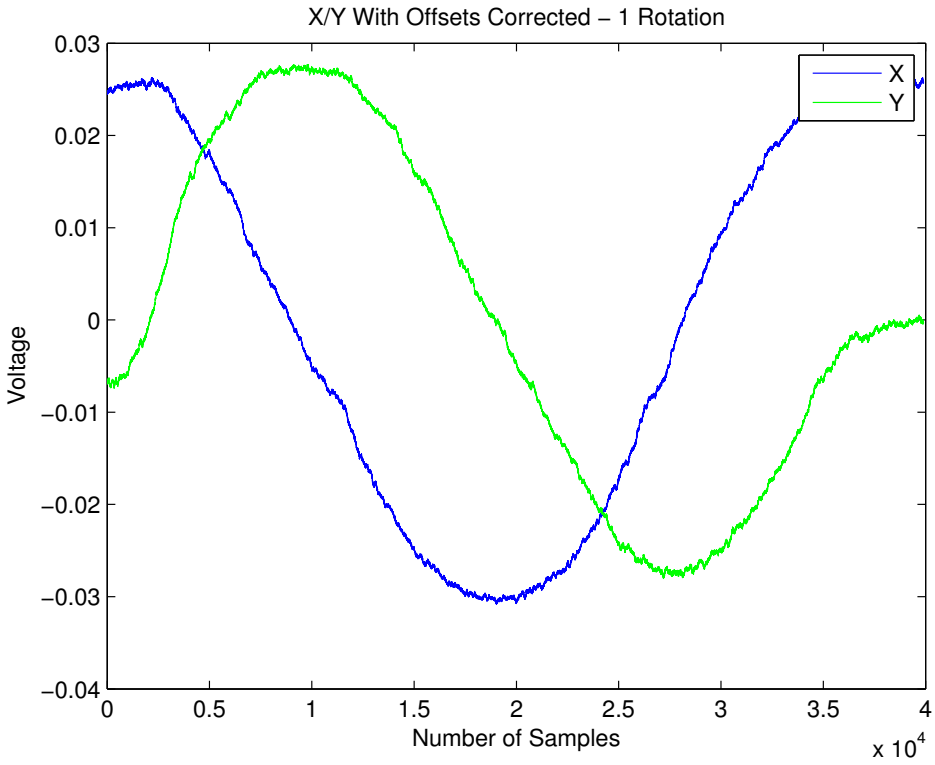

Figure 12: Conditioned X/Y Die Voltages Offset Removed

Figure 13 represents the corrected X and Y values from the compass board. An algorithm constantly runs on the acquired data and checks to see if the minima and maxima of the curves after a calibration rotation change, and if so, the mean is recalculated and the offset corrected.

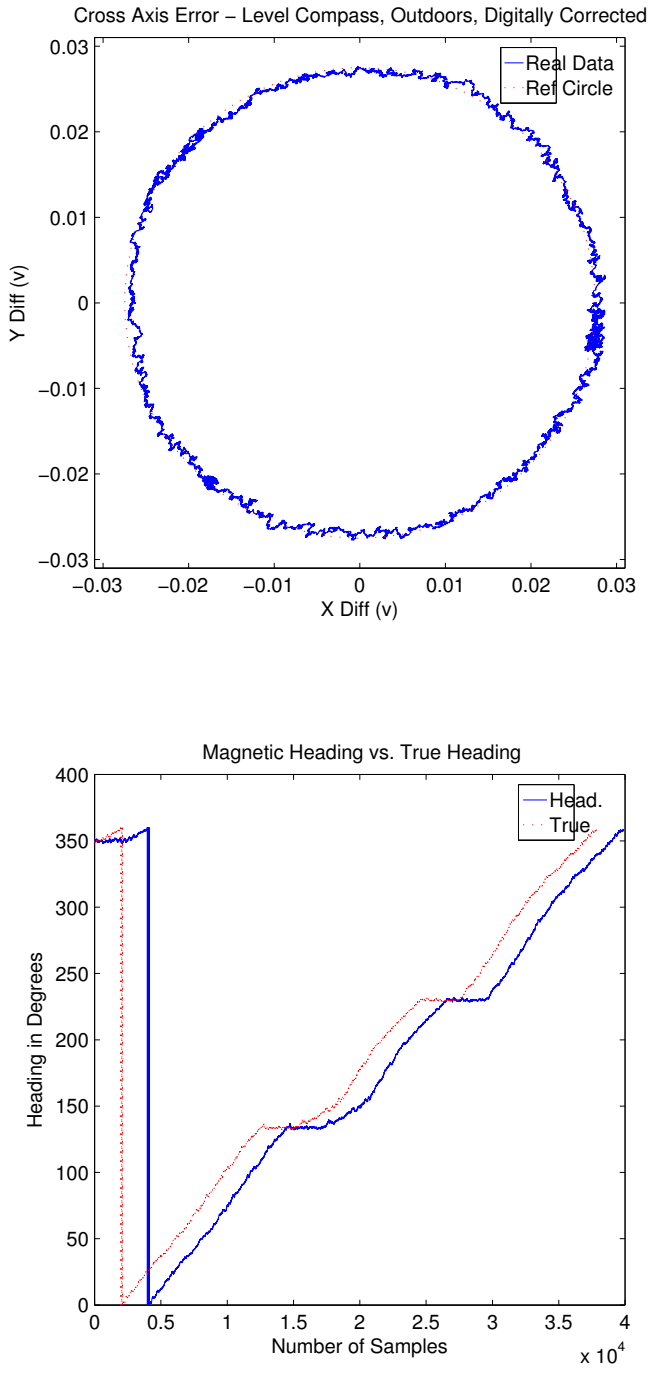

Figure 13: Cross Axis and Heading Error

Figure 14 represents the range of output heading values during a single rotation and its cross-axis error. It should be noted that the cross axis error looks circular in the top graph (a reference circle is included such that if this report is printed in a different aspect ratio the comparison can still be made) and not skewed due to a constant correction digitally subtracted from the X and Y die inputs based off of a statistical characterization of the HMC1022 and its sensitivity.

The bottom graph represents the determined heading versus the true heading. In practice I found that the reported magnetic north reading was 15 degrees SE of north, close to the 14 degree magnetic declination in the earth's magnetic field that we experience in central California. It's also interesting to note that in this data one can see when I switched hads to continue rotating the compass as they read as points where the derivative of the slope goes to zero. (Between $1.4x10^4$ and $2x10^4$ samples is a good example of this.) In this sense the magnetometer is acting as a rotary encoder.

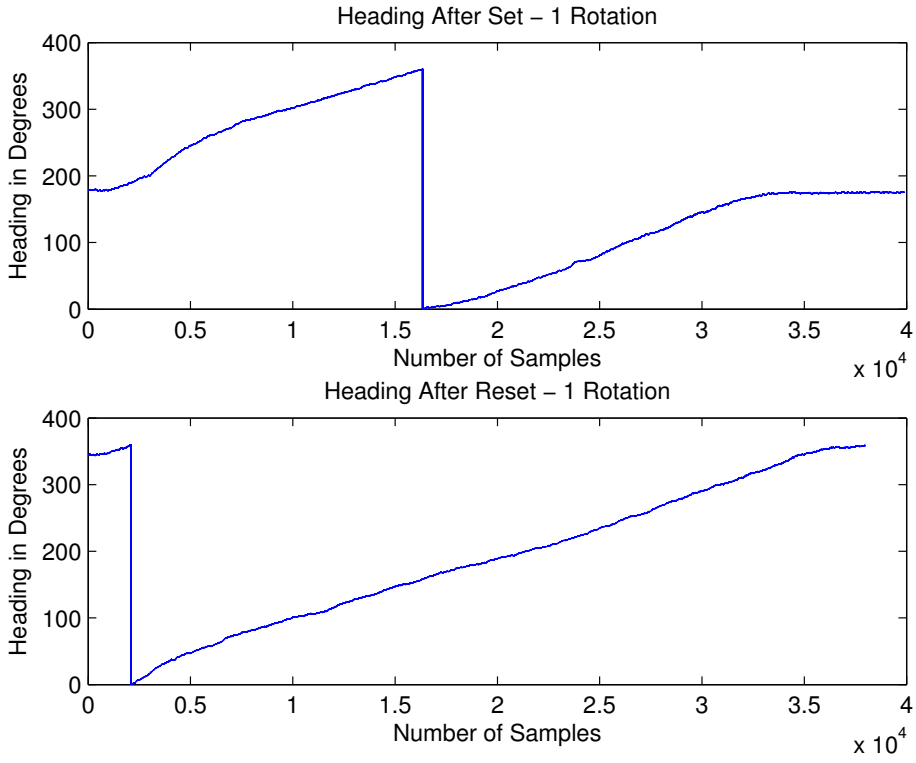

Figure 14: Heading Relation To Set/Reset

Figure 15 represents the reported heading during a set/reset event, and after only a set event over the course of one full rotation. The flipping of the sensitive axis is obvious as the heading changes by a full 180 degrees.

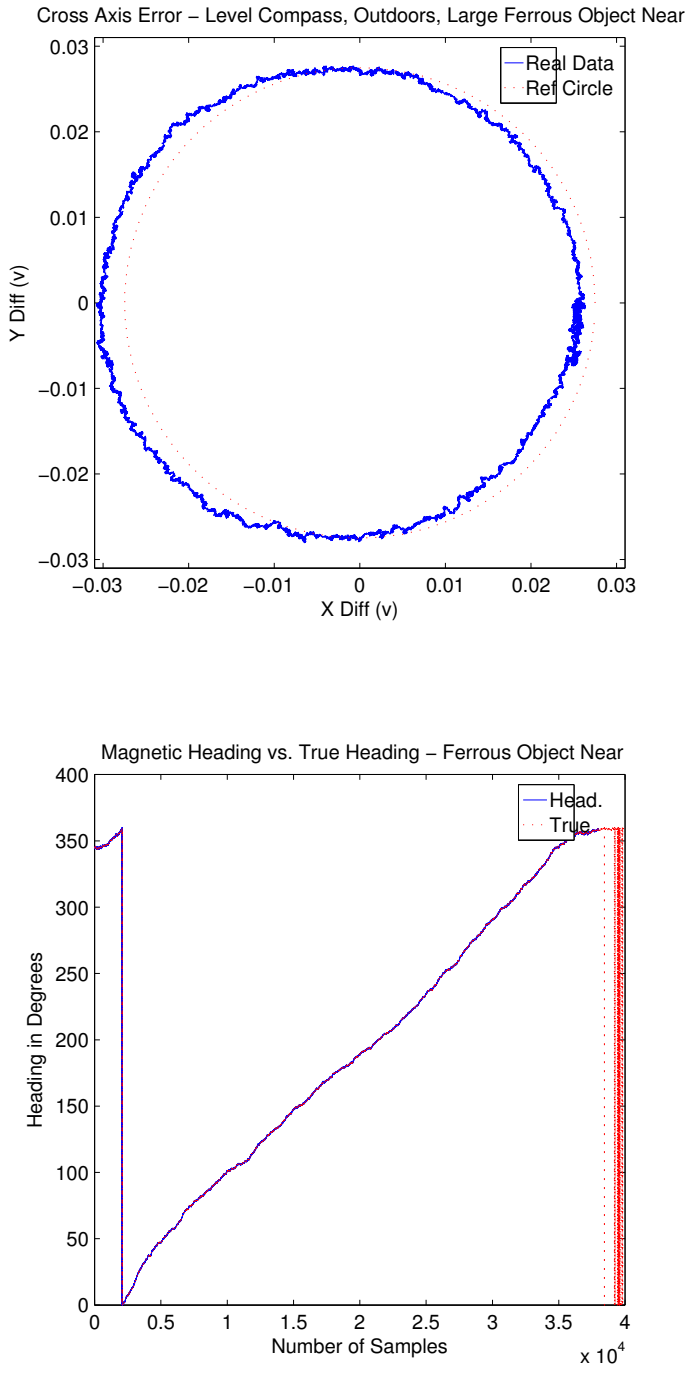

Figure 15: Cross Axis and Heading Error - Offset Due To Large Ferrous Object

Much like in figure 14, figure 16 represents the range of output heading values during a single rotation and its cross-axis error. A large 20 pound permanent magnet motor was placed a foot from the compass board during this run. As a result of this object and its magnetic field being in close proximity to the compass board an offset of 15 degrees was added to the system, this can be seen in the cross-axis error circle and in the Magnetic Heading vs. True Heading graph below it. It was purely coincidence that this object provided the right offset to correct the heading to true north.

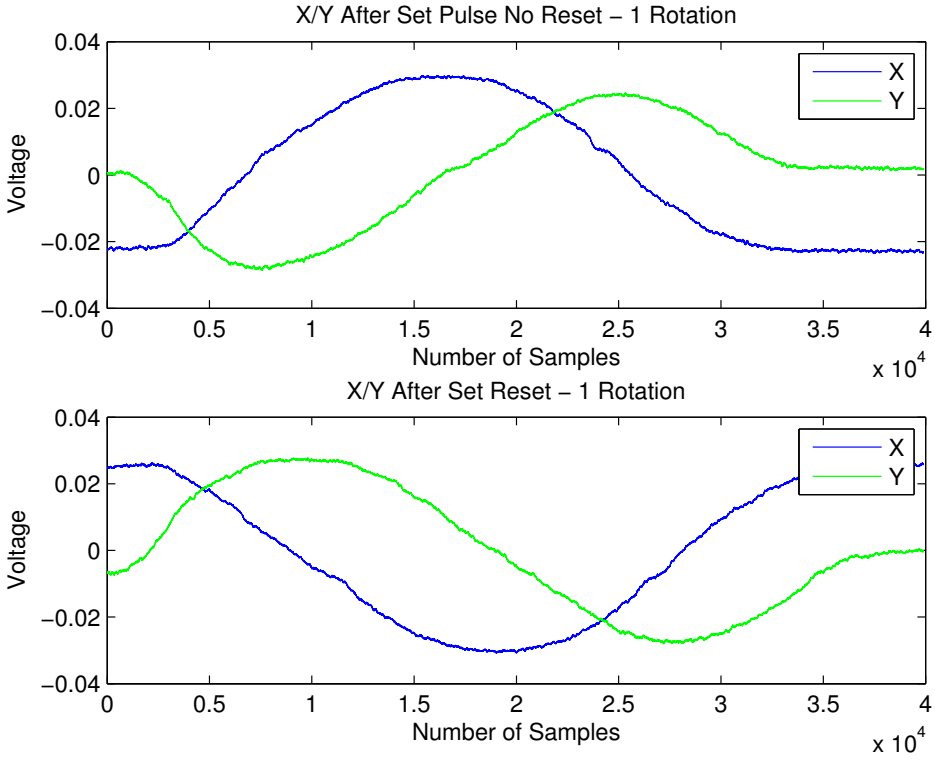

Figure 16: Inverse X/Y Relation With Respect To Set/Reset

Figure 17 represents the X and Y die voltages which created the headings seen in figure 15. Again, a 180 degree shift is apparent as the outputs are inverted.

4 Conclusion

This was an extremely rewarding lab which wrapped together all of the concepts learned in this class ranging from precision op-amp applications, noise analysis, and intelligent sensor systems level engineering to broader topics like magnetic circuits. Even though I spent a solid three hours hardware debugging due to a circuit schematic capture error (non-inverting terminal and inverting terminal swapped on op-amps) I feel as though the lab was fairly straight-forward and did not ask too much of myself or my peers while still challenging us

with an interesting sensor and a practical application.

As I find myself writing the last sentences of this report and I'm free to contemplate my experience with this sensor I'm filled with a strong sense of remorse. A remorse that comes from the realization that the AMR sensor is such a versatile sensor with so many different applications and methods of error correction which I wasn't able to explore fully. If I had not been so obdurate to its intriguing anisotropic wiles due to my resolve to do well on my other finals I'm sure that I would have been able to explore them more fully. That all being said, this lab was a wonderful introduction to this sensor system and I feel much more capable and confident in my abilities to integrate sensors which require a significant amount of analog conditioning and support circuitry into a system.